Clinical SCIENCE

www.clinsci.org

Clinical Science (2010) **118**, 727–736 (Printed in Great Britain) doi:10.1042/CS20090452

Myriocin-mediated up-regulation of hepatocyte apoA-I synthesis is associated with ERK inhibition

Elias N. GLAROS*†, Woojin S. KIM*† and Brett GARNER*†‡

*Prince of Wales Medical Research Institute, Sydney, NSW 2031, Australia, †School of Medical Sciences, Faculty of Medicine, University of New South Wales, Sydney, NSW 2052, Australia, and ‡School of Biological Sciences, University of Wollongong, Wollongong, NSW 2522, Australia

A B S T R A C T

Sphingolipids including sphingomyelin have been implicated as potential atherogenic lipids. Studies in apoE (apolipoprotein E)-null mice have revealed that the serine palmitoyltransferase inhibitor myriocin reduces plasma levels of sphingomyelin, ceramide, sphingosine-1-phosphate and glycosphingolipids and that this is associated with potent inhibition of atherosclerosis. Interestingly, hepatic apoA-I (apolipoprotein A-I) synthesis and plasma HDL (high-density lipoprotein)-cholesterol levels were also increased in apoE-null mice treated with myriocin. Since myriocin is a known inhibitor of ERK (extracellular-signal-related kinase) phosphorylation, we assessed the possibility that myriocin may be acting to increase hepatic apoA-I production via this pathway. To address this, HepG2 cells and primary mouse hepatocytes were treated with 200 μM myriocin for up to 48 h. Myriocin increased apoA-I mRNA and protein levels by approx. 3- and 2-fold respectively. Myriocin also increased apoA-I secretion up to 3.5-fold and decreased ERK phosphorylation by approx. 70%. Similar findings were obtained when primary hepatocytes were isolated from apoE-null mice that were treated with myriocin (intraperitoneal injection at a dose of 0.3 mg/kg body weight). Further experiments revealed that the MEK (mitogen-activated protein kinase/ERK kinase) inhibitor PD98059 potently inhibited ERK phosphorylation, as expected, and increased primary hepatocyte apoA-I production by 3-fold. These results indicate that ERK phosphorylation plays a role in regulating hepatic apoA-I expression and suggest that the anti-atherogenic mechanism of action for myriocin may be linked to this pathway.

INTRODUCTION

Atherosclerosis is a major cause of CVD (cardiovascular disease) and accounts for approx. 50% of all deaths in westernized countries [1]. Hypercholesterolaemia is a major risk factor for atherosclerosis, and it is clear that HMG-CoA (3-hydroxy-3-methylglutaryl-CoA) reductase inhibitors (statins) effectively lower serum total cholesterol and LDL (low-density lipoprotein)-cholesterol levels and reduce cardiovascular morbidity and mortality [2]. However, it is recognized that a significant number of patients are either resistant to or intolerant to statins, and with guidelines for LDL-cholesterol levels to be reduced below 2 mM, it has

Key words: apolipoprotein A-I (apoA-I), atherosclerosis, extracellular-signal regulated kinase (ERK), hepatocyte, myriocin, sphingolipid.

Abbreviations: 4-AAP, 4-aminoantipyrine; apoA-I, apolipoprotein A-I; apoE, apolipoprotein-E; DAOS, *N*-ethyl-*N*-(2-hydroxy-3-sulfopropyl)-3,5-dimethoxyaniline sodium salt; DMEM, Dulbecco's modified Eagle's medium; ERK, extracellular-signal-related kinase; FCS, fetal calf serum; GCS, glucosylceramide synthase; GSL, glycosphingolipid; HDL, high-density lipoprotein; HRP, horseradish peroxidase; i.p., intraperitoneal(ly); LDL, low-density lipoprotein; MAPK, mitogen-activated protein kinase; MEK, MAPK/ERK kinase; MTT, 3-(4,5-dimethylthiazol-2-yl)-2,5-diphenyl-2*H*-tetrazolium bromide; qPCR, quantitative PCR; S1P, sphingosine 1-phosphate; SM, sphingomyelin; SMase, sphingomyelinase; SPT, serine palmitoyltransferase.

Correspondence: Professor Brett Garner (email b.garner@powmri.edu.au).

been reported that less than 50% of patients treated with statins achieve their targets [3]. In order to address this problem, statin combination therapies are under investigation; for example, using the cholesterol absorption inhibitor ezetimibe [3]. We predict that, as an adjunct to statin therapy, approaches targeting pro-atherogenic pathways that are not primarily aimed at reducing cholesterol synthesis or absorption would result in a two-pronged approach to treat atherosclerosis.

Therapeutic targeting of the sphingolipid biosynthetic pathway may represent a feasible approach to treat atherosclerosis [4–7]. Previous studies have shown that plasma SM (sphingomyelin) concentration is an independent risk factor for coronary artery disease [8]. SM is also known to accumulate in atherosclerotic lesions in humans and animal models [9,10]. Similar relationships have been established with plasma GSLs (glycosphingolipids). GSLs are elevated in patients at increased risk of developing atherosclerosis [11], and these sphingolipids accumulate in atherosclerotic lesions in humans and in apoE (apolipoprotein E)$^{-/-}$ mice [12,13]. In addition, several *in vitro* studies have revealed potential atherogenic properties for specific GSLs. These include the findings that LacCer (lactosylceramide) promotes cholesterol accumulation in macrophage foam cells [14], inhibits cellular cholesterol removal via the ABCA1 (ATP-binding cassette, subfamily A, member 1)/apoA-I (apolipoprotein A-I) pathway [15], induces monocyte adhesion to endothelial cells [16] and stimulates vascular smooth muscle cell proliferation [17]. This body of work suggests that sphingolipid synthesis inhibition may be a feasible therapeutic target for the treatment of atherosclerosis.

Several studies have shown that the SPT (serine palmitoyltransferase) inhibitor myriocin is a potent inhibitor of atherosclerosis in apoE$^{-/-}$ mice [18–22]. Myriocin inhibits the initial step in the sphingolipid biosynthetic pathway, which could potentially result in the modulation of several downstream sphingolipid family members. Therefore, the precise mechanism(s) by which myriocin exerts its potent anti-atherogenic action is presently unknown. Myriocin may exert its effects by reducing the concentrations of lipids downstream of ceramide [such as SM, GSLs, C1P (ceramide 1-phosphate) and S1P (sphingosine 1-phosphate)] or by altering the expression of anti-atherogenic genes in the liver. Findings from apoE$^{-/-}$ mouse studies indicate that induction of hepatic apoA-I production is one plausible anti-atherogenic action of myriocin [21,23].

It is widely reported that sphingolipids are critical mediators of intracellular signalling pathways [24–26]. This has lead us to consider signalling pathways that could potentially link the action of myriocin to the increased hepatic apoA-I synthesis we observed *in vivo* [21]. It has been reported that S1P stimulates the phosphorylation of the MAPK (mitogen-activated protein kinase) ERK2 (extracellular-signal-related kinase 2) [27,28]. This activation of ERK2 is mediated by upstream kinases such as MEK (MAPK/ERK kinase), MEK kinase and Raf-1. The phosphorylation of ERK2 leads to dimer formation with other ERK elements. Dimerization leads to translocation to the nucleus where the ERK dimers phosphorylate various transcription factors that can regulate gene expression. Interestingly, it has been established that basal and TNFα (tumour necrosis factor α)-mediated suppression of apoA-I transcription is modulated via an ERK pathway [29] and that myriocin reduces intracellular S1P levels and ERK phosphorylation [30]. This raises the possibility that myriocin may induce apoA-I transcription via down-regulation of ERK phosphorylation. To investigate this possibility, in the current studies, we treated HepG2 cells and primary murine hepatocytes with myriocin or the MEK inhibitor PD98059 and assessed the impact this has on hepatic ERK phosphorylation and apoA-I production.

MATERIALS AND METHODS

Materials

Inhibitor compounds myriocin (cat. no. M1177) and PD98059 (cat. no. P215) were obtained from Sigma. The anaesthetic agent sodium pentobarbitone (cat. no. 35976/01A) was obtained from Rhone Merieux. Inhalation anaesthetic methoxyflurane (cat. no. 43144) was from Medical Developments International. The collagenase mixture Liberase Blendzyme 3 (cat. no. 11814176001) was obtained from Roche. All organic solvents were of analytical grade and were purchased from Ajax Finechem. All other reagents were purchased through standard commercial suppliers.

Cell culture

HepG2 cells were grown under standard culture conditions at 37°C in DMEM (Dulbecco's modified Eagle's medium–low glucose, 1 mg/ml) supplemented with 10% FCS (fetal calf serum), 2 mM glutamine, 50 units/ml penicillin G and 50 μg/ml streptomycin (Invitrogen) in a humidified atmosphere containing 5% CO_2. The cells were subcultivated by trypsinization at a 1:3 ratio and transferred to CellBIND® 12-well cluster plates (cat. no. 3336; Corning) for use in experiments. Primary mouse hepatocytes were isolated from livers obtained from apoE$^{-/-}$ mice and cultured under identical conditions. Cells were treated with myriocin or PD98059 as indicated for up to 48 h. These compounds were added to cells in the absence of serum to enable accurate quantification of secreted apoA-I in culture supernatants.

Myriocin administration and isolation of murine hepatocytes

Male apoE$^{-/-}$ mice were supplied by the Animal Resources Centre. Primary hepatocytes were isolated

[31] from control mice and from mice that were injected i.p. (intraperitoneally) with myriocin (0.3 or 1.0 mg/kg of body weight) three times over 5 days (days 1, 3 and 5) as previously described [20]. Briefly, mice were anaesthetized with sodium pentobarbitone (50 mg/kg of body weight, i.p.) and methoxyflurane (inhalation), and an incision was made down the ventral midline to reveal the viscera. The organs were displaced to allow access to the liver. A ligature was placed around the vena cava upstream of the renal veins and tied off around a 24-gauge catheter inserted into the vena cava downstream of the ligature. A perfusion was initiated (50 ml of Krebs–Ringer containing 20 mM glucose and 0.1 mM EGTA, pH 7.4) at 2 ml/min. The portal vein was then severed, and the flow rate was increased to 7 ml/min. The anterior vena cava was clamped between the diaphragm and heart using a small haemostat. The perfusion was continued with a second buffer (50 ml of Krebs–Ringer containing 20 mM glucose, 1.37 mM $CaCl_2$ and 0.021 mg/ml Liberase Blendzyme 3, pH 7.4). The liver was then excised into a Petri dish with 20 ml of chilled perfusion buffer and ruptured with a scalpel. The cells were dispersed by aspiration through a large-bore pipette and isolated by centrifugation at 100 ***g*** for 5 min at 4 °C. Cells were washed three times with ice-cold culture medium (DMEM). The cells were plated at a density of 1.0×10^6 cells · ml^{-1} · $well^{-1}$. Hepatocytes that were isolated from mice receiving myriocin were analysed in experiments 2 h after plating down. Cell viability exceeded 90 %, as assessed by Trypan Blue staining.

All precautions were taken to ensure that the animals did not suffer unduly during and after the experimental procedure. The work was undertaken with approval from the University of New South Wales Animal Care and Ethics Committee (Approval No. 08/38A).

SM analysis

Analysis of cell lysates for SM was based on a published method [32]. SM measurement involved a four-step enzymatic process, whereby SMase (sphingomyelinase) (cat. no. S-7651; Sigma) hydrolysed SM to phosphorylcholine and *N*-acylsphingosine. Subsequently, alkaline phosphatase (cat. no. P5521; Sigma) generated choline from phosphorylcholine, which in turn was used to generate H_2O_2 in a reaction catalysed by choline oxidase (cat. no. C5896; Sigma). The final step detected liberated H_2O_2 using DAOS [*N*-ethyl-*N*-(2-hydroxy-3-sulfopropyl)-3,5-dimethoxyaniline sodium salt] (cat. no. OC06; Dojindo Molecular Technologies), 4-AAP (4-aminoantipyrine) (cat. no. A4382; Sigma) and HRP (horseradish peroxidase) (cat. no. P1139; Sigma) to generate a blue dye. The reaction buffer components were prepared in 0.05 M Tris/HCl and 0.66 mM calcium chloride, pH 8. Enzyme concentrations in a 10-ml reaction buffer were as follows: 5 units of SMase, 100 units of alkaline phosphatase, 5 units of choline oxidase and 200 units of HRP. 4-AAP and DAOS concentrations were both 0.73 mM. Cell lysate (5 μl) was added to 100 μl of reaction buffer and, after 45 min of incubation at 37 °C, the absorption was measured at 595 nm using a spectrophotometric plate reader (Model 550; Bio-Rad Laboratories). A standard curve was prepared using aliquots of a stock SM solution (1 mg/ml) prepared by dissolving 10 mg of SM in 10 ml of 2 % (w/v) Triton X-100 in ethanol.

Real-time qPCR (quantitative PCR) analysis of HepG2 cell and primary murine hepatocyte apoA-I mRNA

RNA was isolated from the cell monolayers using TRIzol® reagent (Invitrogen) according to the manufacturer's protocol. All procedures were carried out using RNase-free reagents. RNA was reverse-transcribed into cDNA using MMLV (Moloney-murine-leukaemia virus) reverse transcriptase and random primers (Promega). cDNA generated from the reverse transcription of total RNA was used as a template in the qPCR assay. qPCR amplification was carried out using a Mastercycler ep realplex S (Eppendorf) and the fluorescent dye SYBR Green (Eppendorf) according to the manufacturer's protocol. Briefly, each reaction (20 μl) contained 20 pmol of primers, 1× Real MasterMix, 0.5× SYBR Green and 1 μl of template. Amplification was carried out with 40 cycles of denaturation (94 °C, 30 s), annealing (57 °C, 30 s) and extension (72 °C, 30 s). All gene expressions were normalized to β-actin or Gapdh (glyceraldehyde-3-phosphate dehydrogenase). The primer sequences (5′–3′) and PCR product sizes are as follows: human apoA-I (234 bp) forward, CTTGGCCGTGCTCTTCCTGAC, and reverse, TTCCCGTTCTCAGCCTTGAC; human β-actin (162 bp) forward, GAATTCTGGCCACGGCTGCTTCCAGCT, and reverse, AAGCTTTTTCGTGGATGCCACAGGACT; mouse apoA-I (129 bp) forward, GGCACGTATGGCAGCAAGAT, and reverse, CCAAGGAGGAGGATTCAAACTG; mouse Gapdh (83 bp) forward, TGGTGAAGCAGGCATCTGAG, and reverse, TGCTGTTGAAGTCGCAGGAG.

Western blot analysis of HepG2 cells and mouse primary hepatocytes

Cell monolayers were lysed in 400 μl of RIPA buffer [20 mM Tris/HCl, pH 7.5, 150 mM NaCl, 1 mM EDTA, 1 % Nonidet P40, 0.5 % deoxycholate, 0.1 % SDS and protease inhibitors (cat. no. 11836153001; Roche)]. Culture supernatant samples were also collected. Lysate (32 μl) was mixed with 8 μl of 5× Laemmli sample buffer and 30 μl was routinely used for SDS/PAGE and Western blotting. Culture supernatant (36 μl) was mixed with 9 μl of 5× Laemmli sample buffer and 40 μl was loaded on to gels. All samples were heated at 95 °C for 5 min and briefly centrifuged before loading. Samples were separated by

SDS/PAGE (12% gels) using a Bio-Rad Laboratories mini-gel system. The proteins were transferred on to 0.45 μm Trans-Blot nitrocellulose membranes (cat. no. 162-0115; Bio-Rad Laboratories), and the membranes were probed with a 1:2000-diluted rabbit anti-(human apoA-I) polyclonal antibody that cross-reacts strongly with mouse apoA-I (cat. no. 178422; Calbiochem) and detected with 1:2000-diluted HRP-conjugated anti-rabbit secondary antibody (cat. no. 2012-09; DAKO) and ECL (enhanced chemiluminescence) advanced detection reagents (GE Healthcare). Membranes were also probed with rabbit anti-ERK1/2 polyclonal (cat. no. 9102; Cell Signaling Technology) or mouse anti-phospho-ERK1/2 polyclonal (cat. no. 442706; Calbiochem) antibodies, both used at 1:2000 dilutions. Blots were also probed for β-actin using rabbit anti-actin polyclonal antibodies (cat. no. 057K4856; Sigma) to confirm equal protein loading. The intensity of the protein bands was measured using ImageJ software, which is available in the public domain (http://rsb.info.nih.gov/ij/).

Cell viability assay

Primary mouse hepatocytes were seeded into 96-well plates at 80% confluency. Cells were treated with the indicated doses of myriocin for 48 h. The culture medium was removed, and 100 μl of medium (DMEM and 10% FCS) containing 0.5 mg/ml MTT [3-(4,5-dimethylthiazol-2-yl)-2,5-diphenyl-2*H*-tetrazolium bromide] (cat. no. M2128; Sigma) was added, and cells incubated for 3 h at 37°C. The medium was discarded and cells were dissolved in DMSO (100 μl/well), and the absorbance of the cell lysates was measured at 550 nm. Higher absorbance values indicate increased cell viability.

Statistics

All results are presented as means ± S.E.M. of triplicate or quadruplicate samples with experiments routinely repeated three times. Statistical significance for differences in mRNA and protein levels was determined using a Student's *t* test. Differences were considered significant at $P < 0.05$.

RESULTS

It has been shown previously that SPT inhibition can reduce cellular S1P levels and ERK2 phosphorylation [30]. In the current study, 100 and 200 μM myriocin were applied to HepG2 cells and primary hepatocytes for up to 48 h to determine its affect on apoA-I levels and ERK phosphorylation. In HepG2 cells, myriocin increased apoA-I mRNA levels 2.5-fold over controls after 24 h. This was extended to a 3-fold increase after 48 h incubation (Figure 1A). This increase was also reflected at the protein level, although the increase was not as dramatic, with intracellular apoA-I protein levels raised by 1.4-fold. ApoA-I secretion also increased by 1.3-fold (Figures 1B and 1C). This was repeated using 200 μM myriocin and the membrane probed for total ERK and phospho-ERK, as well as apoA-I (Figure 2). Once again, apoA-I protein levels were increased ~1.4-fold. ERK phosphorylation was reduced by ~50%, with total ERK levels remaining unchanged. This indicates that reduced phospho-ERK levels are not due to reduced levels of total ERK. All protein levels were normalized to β-actin. The impact of myriocin on apoA-I mRNA levels was also analysed by qPCR, and a 2-fold increase was demonstrated (Figure 2B).

In order to use *in vitro* conditions that more closely resemble the *in vivo* experiments in which myriocin has been shown to potently inhibit atherosclerosis [20], we focused on the study of primary hepatocytes. The experiments using the HepG2 hepatocarcinoma cell line were replicated using primary mouse hepatocytes under identical conditions. Primary hepatocytes were treated with 200 μM myriocin for 24 h. In a similar fashion to HepG2 cells, myriocin increased apoA-I protein levels 1.6-fold over controls. ApoA-I secretion also increased 2.4-fold. Furthermore, myriocin increased apoA-I mRNA levels ~3-fold (Figure 3). This was repeated in a separate series of experiments and the membranes probed for total ERK, phospho-ERK, as well as apoA-I. Cell supernatants were also assessed for apoA-I secretion (Figure 4A). Cellular apoA-I protein levels were increased 1.7-fold, with secreted apoA-I increasing 3.4-fold (Figure 4B). ERK phosphorylation was reduced by 72%, with total ERK and β-actin levels remaining unchanged. Again, myriocin increased apoA-I mRNA levels 2-fold (Figure 4B).

ERK activation is a rapidly inducible and dynamic process. We therefore also assessed earlier time points (<24 h) to examine if apoA-I expression can be rapidly induced by 200 μM myriocin. The results indicate that there was no induction of apoA-I mRNA after 1 h (Figure 5A). A moderate (40%) increase in apoA-I mRNA was detected after 6 h, and strong induction (2.3-fold) was observed at 24 h (Figure 5A). Although a consistent significant myriocin-mediated induction of cellular and secreted apoA-I protein levels was observed by 24 h (as shown above), no consistent up-regulation of apoA-I protein levels was detected at the 1 and 6 h time points (results not shown). We did not detect any significant changes in β-actin levels even at the highest myrocin dose used (200 μM) after 48 h. In order to check for possible cytotoxic/cytostatic properties that may be associated with myriocin, an MTT reduction assay for cell viability was also conducted using primary hepatocytes treated with various doses of myriocin for 48 h. The results indicate that there was a moderate (10% to 19%) but statistically significant decrease in MTT reduction in cells treated with either 100 or 200 μM myriocin

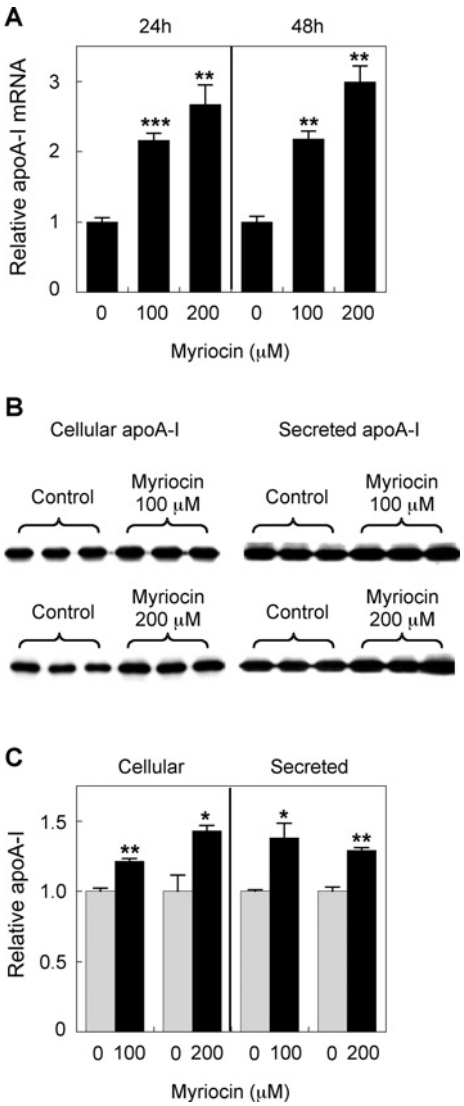

Figure 1 Myriocin up-regulates HepG2 cell apoA-I production

(A) HepG2 cells were treated with 100 or 200 μM myriocin for 24 or 48 h, and mRNA expression was assessed by qPCR. (B and C) HepG2 cells were treated with 100 or 200 μM myriocin for 24 h. The cell medium was collected after 24 h, and apoA-I expression and secretion were analysed by Western blotting. Signal intensity of the apoA-I bands was quantified using Image-J software and the results are expressed relative to controls. Results are means $\pm$ S.E.M. $^{*}P < 0.05$, $^{**}P < 0.01$ and $^{***}P < 0.0001$ as assessed by Student's *t* test.

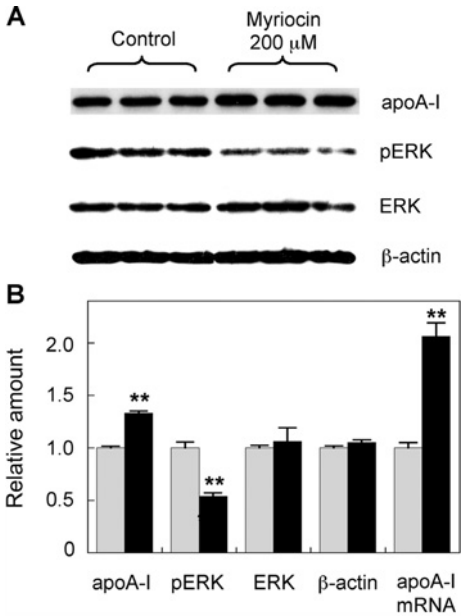

Figure 2 Myriocin-mediated up-regulation of HepG2 cell apoA-I production is associated with inhibition of ERK phosphorylation

(A) HepG2 cells were treated with 200 μM myriocin for 24 h, and apoA-I, ERK, phospho-ERK (pERK) and β-actin levels were analysed by Western blotting. (B) Signal intensity of the bands quantified by Image-J software. Analysis of apoA-I mRNA expression via qPCR was performed under identical conditions. Grey bars, control; black bars, myriocin-treated. Results are means $\pm$ S.E.M. $^{**}P < 0.01$ as assessed by Student's *t* test.

for 48 h (Figure 5B). This indicates that, although myriocin does appear to have a moderate impact on cellular MTT reduction, viability remained high, and the myriocin-mediated induction of hepatocyte apoA-I is not likely to be due to non-specific cytotoxic effects of the drug.

The extent of myriocin-mediated inhibition of SPT activity in both HepG2 cells and primary murine hepatocytes was confirmed by measurement of SM levels in cell lysates. The results indicated that 24 h treatment with 200 μM myriocin reduced HepG2 cell and primary hepatocyte SM levels by 47% and 38% respectively (Figure 6). The extent of SM depletion observed in these *in vitro* experiments is similar to the reductions achieved in our previous *in vivo* studies. When apoE$^{-/-}$ mice were treated with myriocin by either i.p. injection or oral administration, decreases in plasma SM of 42% and 54% respectively, were achieved [20,21]. Of more relevance to the hepatocyte, chronic administration of myriocin to apoE$^{-/-}$ mice reduced hepatic SM levels by (39%) [20,21].

We next examined whether myriocin could induce apoA-I expression and inhibit ERK activation in hepatocytes isolated from mice that were acutely treated with myriocin. In this experiment, mice were injected i.p. with myriocin three times at either 0.3 or 1.0 mg/kg of body weight over 5 days (i.e. injected on days 1, 3 and 5). Approximately 2 h after the final injection, hepatocytes were isolated and plated out as described in the Materials and methods section. At 2 h after plating, the cells were harvested and assessed for apoA-I and ERK/phospho-ERK expression (secreted apoA-I protein levels could not be reliably quantified by Western blotting in the medium taken from freshly isolated hepatocytes

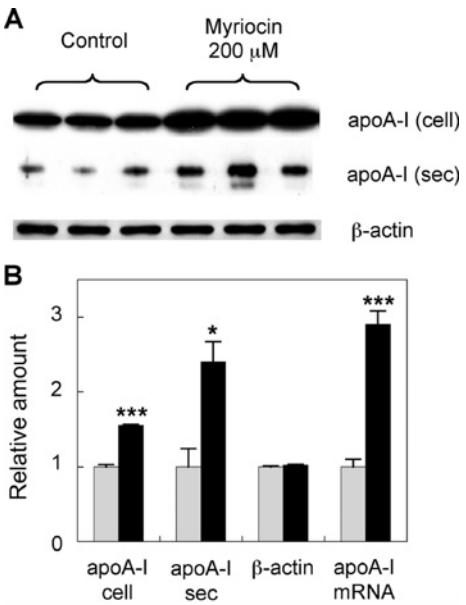

Figure 3 Myriocin up-regulates mouse hepatocyte apoA-I production

(A) Primary hepatocytes were treated with 200 μM myriocin for 24 h. ApoA-I and β-actin levels were analysed by Western blotting. (B) Signal intensity of the bands was quantified using Image-J software. Analysis of apoA-I mRNA expression via qPCR was performed under identical conditions. Grey bars, control; black bars, myriocin-treated. Results are means $\pm$ S.E.M. $^{*}P < 0.05$ and $^{***}P < 0.0001$ as assessed by Student's t test. cell, cellular, sec, secreted.

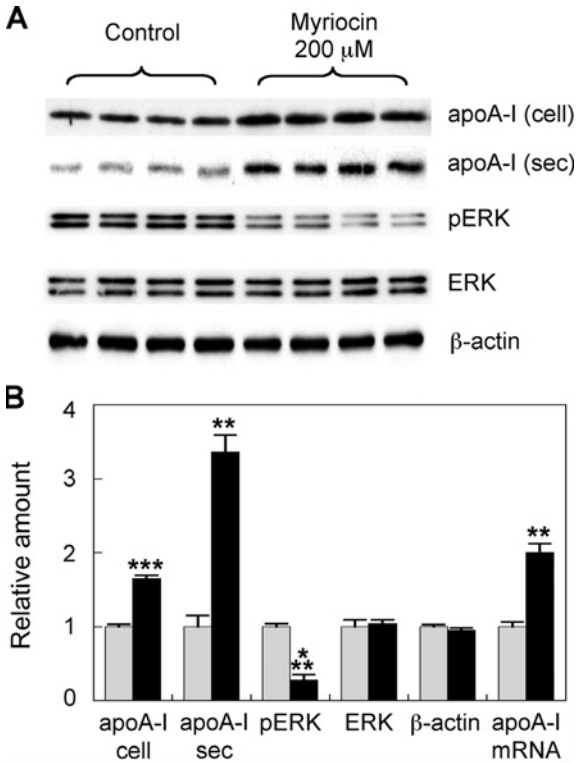

Figure 4 Myriocin-mediated up-regulation of mouse hepatocyte apoA-I is associated with inhibition of ERK phosphorylation

(A) Primary mouse hepatocytes were treated with 200 μM myriocin for 24 h. The medium was collected after 24 h. Cellular apoA-I (cell) ERK, phospho-ERK (pERK) and β-actin and secreted apoA-I (sec) levels were analysed by Western blotting. (B) Signal intensity of the bands quantified using Image-J. Analysis of apoA-I mRNA expression via qPCR was performed under identical conditions. Grey bars, control; black bars, myriocin-treated. Results are means $\pm$ S.E.M. $^{**}P < 0.01$ and $^{***}P < 0.0001$ as assessed by Student's t test.

that were plated down for only 2 h; results not shown). Hepatocytes derived from mice treated with myriocin at a dose of 0.3 mg/kg of body weight had 1.72- and 1.92-fold increased levels of apoA-I protein and mRNA respectively, compared with PBS-injected control mice (Figure 7). Interestingly, there was no further induction of hepatocyte apoA-I in animals treated with the higher dose (1 mg/kg of body weight) of myriocin. We also detected a moderate 25% inhibition of hepatocyte phospho-ERK in the myriocin-treated mice (Figure 7). These results indicate that the association of myriocin-mediated stimulation of apoA-I synthesis with decreased ERK activation is relevant to both the *in vitro* and *in vivo* experimental settings.

The myriocin-mediated inhibition of hepatocyte ERK phosphorylation we identified suggests that modulation of the ERK pathway may be directly involved in the up-regulation of hepatic apoA-I synthesis. However, it is also possible that the inhibition of ERK phosphorylation by myriocin is merely coincidental with up-regulated apoA-I production. To further understand the link between apoA-I transcription and ERK phosphorylation, we treated mouse hepatocytes with 50 μM PD98059. PD98059 is a potent inhibitor of MEK, the kinase that activates ERK. The cell lysates and supernatants were collected and analysed by SDS/PAGE and Western blotting as above. ERK phosphorylation was reduced by 89%, with total ERK and β-actin levels remaining unchanged (Figure 8A). Cellular and secreted apoA-I protein levels were increased 1.3- and 3.3-fold respectively (Figure 8A). A modest but statistically significant increase in apoA-I mRNA level was also detected (Figure 8B). This adds further support to our proposal that myriocin-mediated inhibition of ERK phosphorylation plays a role in the up-regulation of hepatocyte apoA-I production.

DISCUSSION

We have previously shown that the SPT inhibitor myriocin significantly inhibits atherosclerosis in apoE$^{-/-}$ mice [20,21]. As predicted, this was associated with significant reductions in plasma SM concentrations. We also reported that the anti-atherogenic activity of

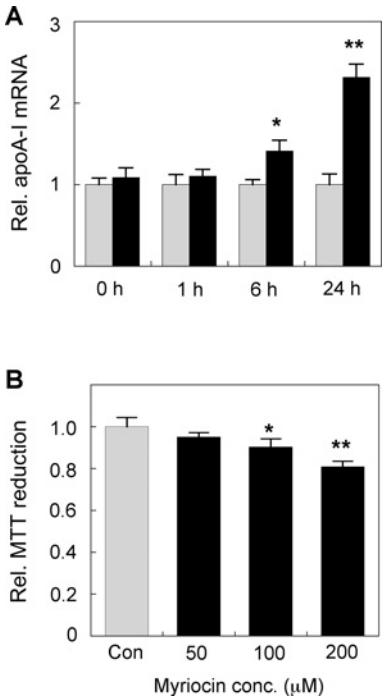

Figure 5 Time course study of myriocin-mediated up-regulation of mouse hepatocyte apoA-I mRNA and its impact on cell viability

(A) Primary mouse hepatocytes were treated with 200 μM myriocin for 0 to 24 h. Cells were extracted in TRIzol® reagent, and apoA-I mRNA expression was assessed by qPCR. (B) Primary mouse hepatocytes were treated with 200 μM myriocin 48 h and cell viability assessed using the MTT reduction assay. Grey bars, control; black bars, myriocin-treated. Results are means $\pm$ S.E.M. $^{**}P < 0.01$ and $^{***}P < 0.0001$ as assessed by Student's t test.

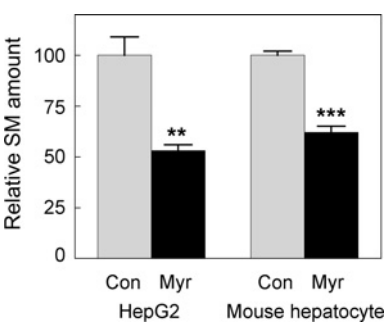

Figure 6 Myriocin decreases SM levels in mouse hepatocytes and HepG2 cells

Cell lysate (5 μl) was added to a 95-μl reaction buffer (see Materials and methods section for details) and, after 45 min of incubation at 37 °C, the absorbance was measured at 595 nm using a spectrophotometric plate reader. The absolute value for total SM, represented by the 100% relative SM, amount for hepatocytes, was 1.20 $\pm$ 0.02 nmol/mg of cell protein. Grey bars, control; black bars, myriocin-treated. Results are means $\pm$ S.E.M. $^{**}P < 0.01$ and $^{***}P < 0.0001$ as assessed by Student's t test.

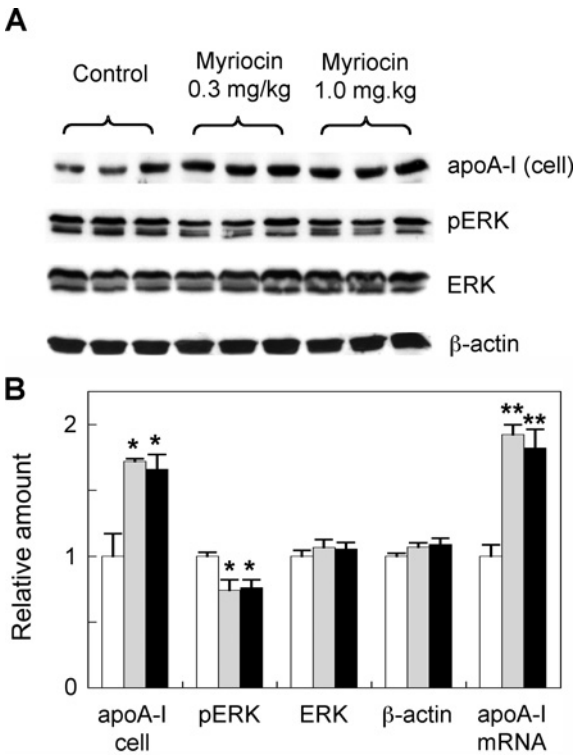

Figure 7 Analysis of apoA-I and ERK levels in hepatocytes derived from myriocin-treated mice

(A) ApoE$^{-/-}$ mice were injected i.p. with myriocin at 0.3 or 1 mg/kg of body weight or PBS as a vehicle control, as described in the Materials and methods section. The animals were killed, and primary hepatocytes were isolated and assessed for apoA-I, ERK, phospho-ERK (pERK) and β-actin by Western blotting. (B) Signal intensity of the bands was quantified by Image-J software and analysis of apoA-I mRNA expression via qPCR was performed under identical conditions. White bars, control; grey bars, 0.3 mg/kg myriocin-treated; black bars, 1 mg/kg myriocin-treated. Results are means $\pm$ S.E.M. of three mice in each treatment group. $^{*}P < 0.05$ and $^{**}P < 0.01$ as assessed by Student's t test.

myriocin was associated with a 29% reduction in plasma GSL levels [20]. The fact that SPT inhibition may have an impact on numerous members of the sphingolipid family, which could theoretically regulate lesion development [7], led us to examine the selective inhibition of GCS (glucosylceramide synthase, which catalyses the initial step in GSL biosynthesis) as a potential modulator of atherosclerosis in apoE$^{-/-}$ mice. In the latter study, we employed the GSL synthesis inhibitor EtDO-P4 (D-*threo*-1-ethylendioxyphenyl-2-palmitoylamino-3-pyrrolidino-propanol), and observed that over a 4-month period on a high-fat/high-cholesterol diet, a 49% reduction in plasma GSL levels ($P < 0.0001$) was achieved by drug administration. However, this was not associated with a significant reduction in atherosclerosis [33,34]. Interestingly, a recent report suggests that another GCS inhibitor, *N*-(5-adamantane-1-yl-methoxy-pentyl)-deoxynojirimycin, significantly reduces atherosclerosis in the APOE*3 Leiden mouse

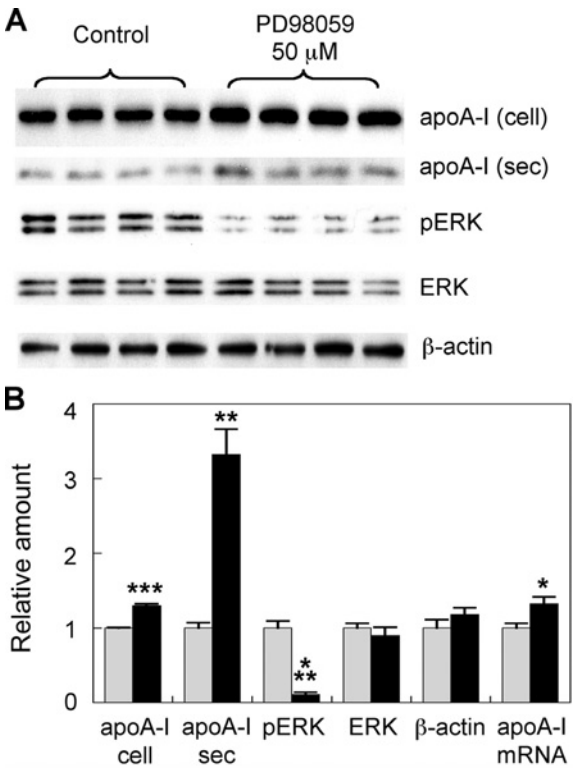

Figure 8 Inhibition of ERK phosphorylation up-regulates mouse hepatocyte apoA-I production

(A) Primary hepatocytes were treated with 50 μM PD98059 for 24 h. The medium was collected after 24 h. Cellular apoA-I (cell), ERK, phospho-ERK (pERK) and β-actin and secreted apoA-I (sec) levels were analysed by Western blotting. (B) Signal intensity of the bands was quantified by Image-J software. Analysis of apoA-I mRNA expression via qPCR was performed under identical conditions. Grey bars, control; black bars, myriocin-treated. Results are means $\pm$ S.E.M. $^{*}P < 0.05$, $^{**}P < 0.01$ and $^{***}P < 0.0001$ as assessed by Student's t test.

model of atherosclerosis [35]. Therefore, it remains possible that myriocin-mediated inhibition of GSL synthesis does contribute to its anti-atherogenic activity [20].

Regardless of the impact on GSL synthesis, myriocin also increases hepatic and plasma apoA-I levels by 45 % and 38 % respectively, in apoE$^{-/-}$ mice [21]. This has also been previously reported in a study showing that apoE$^{-/-}$ mice treated with myriocin at a concentration of 1 mg^{-1} · kg^{-1} of body weight · day^{-1} by oral gavage for 5 days increased hepatic apoA-I mRNA expression by 30 % [23]. Since raising plasma apoA-I levels by pharmacological means has been a major research focus for some time [36], our current objective was to gain information on the underlying mechanism(s) by which myriocin may induce apoA-I expression. This information was also sought in order to help explain its anti-atherogenic actions *in vivo*.

Myriocin reduces plasma S1P concentration in association with inhibition of atherosclerosis in apoE$^{-/-}$ mice [19]. Given that S1P has been shown to stimulate ERK phosphorylation, and that ERK activation has been implicated in the suppression of apoA-I transcription [29,30], we hypothesized that myriocin may induce hepatic apoA-I synthesis through an inhibition of the ERK signalling pathway. Our findings clearly support this hypothesis by showing that myriocin significantly raises apoA-I mRNA and protein levels in both HepG2 cells and primary mouse hepatocytes in association with an inhibition of ERK phosphorylation. Furthermore, we observed a similar up-regulation of apoA-I synthesis and suppression of ERK activation in hepatocytes derived from mice that were treated with myriocin. The role of suppressed ERK signalling in the mechanisms underlying myriocin-mediated up-regulation of hepatic apoA-I production is also supported by our results showing that selective inhibition of ERK phosphorylation with PD98059 significantly increased apoA-I mRNA and protein levels in primary hepatocytes. Importantly, this was associated with a significant increase in hepatocyte apoA-I secretion as well.

The question now arises as to the therapeutic relevance of these observations. As far as we are aware, selective targeting of hepatic ERK phosphorylation has not been previously studied as means to increase plasma apoA-I or HDL (high-density lipoprotein) levels in humans. However, there is one clinical scenario that may have a bearing on our current findings. It is recognized that patients treated with the antipsychotic dibenzodiazepines olanzapine and the closely related clozapine can develop a dyslipidaemia that is characterized by increased total plasma cholesterol and triacylglycerol (triglyceride) levels and decreased HDL-cholesterol and apoA-I levels [37–39]. Intriguingly, clozapine was recently shown to stimulate ERK phosphorylation [40], an event that we would speculate could result in suppression of hepatic apoA-I synthesis. Whether a compound such as myriocin could be utilized to ameliorate the unwanted side effects that dibenzodiazepines have on plasma HDL-cholesterol levels remains to be examined. It is important to note that the influence of dibenzodiazepines on weight gain may also independently result in lowered HDL-colesterol levels, and it would therefore be premature to ascribe antipsychotic drug-induced changes in hepatic ERK activation as the cause of lowered HDL-C in human patients.

Other studies in humans have examined the immunosuppressive function of a myriocin-based drug FTY720 [41]. FTY720 is an S1P homologue that, after *in vivo* phosphorylation, acts as an agonist of G-protein-coupled sphingolipid receptors. Previous studies in LDLr (LDL receptor)$^{-/-}$ mice and apoE$^{-/-}$ mice have shown that FTY720 inhibits atherosclerosis in both these animal models; however, the anti-atherogenic action of FTY720 was not associated with increased HDL levels [42,43]. Consistent with this, we found that FTY720 did not alter

hepatocyte apoA-I synthesis (E. Glaros and B. Garner, unpublished work). The anti-atherogenic mechanisms of action for myriocin and FTY720 therefore appear to be quite distinct. Previous studies have indicated that myriocin may regulate the synthesis of multiple classes of sphingolipids including ceramides and GSLs [7]. Although we have shown that selective GSL inhibition does not affect overall plasma lipid profiles in apoE$^{-/-}$ mice [34], we cannot rule out a possible role for altered levels of GSLs, ceramides or other sphingolipid species as contributing to the pathways by which myriocin induces hepatic apoA-I synthesis.

In conclusion, our results extend existing current knowledge in the area of sphingolipid inhibitors for the treatment of atherosclerosis by demonstrating that an up-regulation of hepatic apoA-I synthesis by myriocin is associated with inhibition of ERK phosphorylation. Identification of specific therapeutic targets in the sphingolipid biosynthetic pathway could lead to novel approaches that may be used in isolation or in conjunction with cholesterol-lowering therapies to better treat atherosclerosis.

FUNDING

This work was supported by a Goldstar Research Award from the University of New South Wales (UNSW). E.N.G. is supported by a UNSW University Postgraduate Award Ph.D. scholarship. B.G. is supported by a Fellowship from the Australian Research Council [grant number FT0991986].

REFERENCES

1 Lusis, A. J. (2000) Atherosclerosis. Nature **407**, 233–241
2 Ballantyne, C. M., Herd, J. A., Dunn, J. K., Jones, P. H., Farmer, J. A. and Gotto, Jr, A. M. (1997) Effects of lipid lowering therapy on progression of coronary and carotid artery disease. Curr. Opin. Lipidol. **8**, 354–361
3 Ballantyne, C. M. (2005) Rationale for targeting multiple lipid pathways for optimal cardiovascular risk reduction. Am. J. Cardiol. **96**, 14K–19K
4 Chatterjee, S. (1998) Sphingolipids in atherosclerosis and vascular biology. Arterioscler. Thromb. Vasc. Biol. **18**, 1523–1533
5 Auge, N., Negre-Salvayre, A., Salvayre, R. and Levade, T. (2000) Sphingomyelin metabolites in vascular cell signaling and atherogenesis. Prog. Lipid. Res. **39**, 207–229
6 Levade, T., Auge, N., Veldman, R. J., Cuvillier, O., Negre-Salvayre, A. and Salvayre, R. (2001) Sphingolipid mediators in cardiovascular cell biology and pathology. Circ. Res. **89**, 957–968
7 Kim, W. S., Chalfant, C. E. and Garner, B. (2006) Fine tuning therapeutic targeting of the sphingolipid biosynthetic pathway to treat atherosclerosis. Curr. Vasc. Pharmacol. **4**, 151–154
8 Jiang, X. C., Paultre, F., Pearson, T. A., Reed, R. G., Francis, C. K., Lin, M., Berglund, L. and Tall, A. R. (2000) Plasma sphingomyelin level as a risk factor for coronary artery disease. Arterioscler. Thromb. Vasc. Biol. **20**, 2614–2618
9 Kummerow, F. A., Cook, L. S., Wasowicz, E. and Jelen, H. (2001) Changes in the phospholipid composition of the arterial cell can result in severe atherosclerotic lesions. J. Nutr. Biochem. **12**, 602–607
10 Smith, E. B. (1960) Intimal and medial lipids in human aortas. Lancet **i**, 799–803
11 Dawson, G., Kruski, A. W. and Scanu, A. M. (1976) Distribution of glycosphingolipids in the serum lipoproteins of normal human subjects and patients with hypo- and hyperlipidemias. J. Lipid Res. **17**, 125–131
12 Breckenridge, W. C., Halloran, J. L., Kovacs, K. and Silver, M. D. (1975) Increase of gangliosides in atherosclerotic human aortas. Lipids **10**, 256–259
13 Garner, B., Priestman, D. A., Stocker, R., Harvey, D. J., Butters, T. D. and Platt, F. M. (2002) Increased glycosphingolipid levels in serum and aortae of apolipoprotein E gene knockout mice. J. Lipid Res. **43**, 205–214
14 Garner, B., Mellor, H. R., Butters, T. D., Dwek, R. A. and Platt, F. M. (2002) Modulation of THP-1 macrophage and cholesterol-loaded foam cell apolipoprotein-E levels by glycosphingolipids. Biochem. Biophys. Res. Commun. **290**, 1361–1367
15 Glaros, E. N., Kim, W. S., Quinn, C. M., Wong, J., Gelissen, I., Jessup, W. and Garner, B. (2005) Glycosphingolipid accumulation inhibits cholesterol efflux via the ABCA1/apoA-I pathway. 1-Phenyl-2-decanoylamino-3-morpholino-1-propanol is a novel cholesterol efflux accelerator. J. Biol. Chem. **280**, 24515–24523
16 Gong, N., Wei, H., Chowdhury, S. H. and Chatterjee, S. (2004) Lactosylceramide recruits PKCα/ε and phospholipase A2 to stimulate PECAM-1 expression in human monocytes and adhesion to endothelial cells. Proc. Natl. Acad. Sci. U.S.A. **101**, 6490–6495
17 Bhunia, A. K., Han, H., Snowden, A. and Chatterjee, S. (1997) Redox-regulated signaling by lactosylceramide in the proliferation of human aortic smooth muscle cells. J. Biol. Chem. **272**, 15642–15649
18 Park, T. S., Panek, R. L., Mueller, S. B., Hanselman, J. C., Rosebury, W. S., Robertson, A. W., Kindt, E. K., Homan, R., Karathanasis, S. K. and Rekhter, M. D. (2004) Inhibition of sphingomyelin synthesis reduces atherogenesis in apolipoprotein E-knockout mice. Circulation **110**, 3465–3471
19 Hojjati, M. R., Li, Z., Zhou, H., Tang, S., Huan, C., Ooi, E., Lu, S. and Jiang, X. C. (2005) Effect of myriocin on plasma sphingolipid metabolism and atherosclerosis in apoE-deficient mice. J. Biol. Chem. **280**, 10284–10289
20 Glaros, E. N., Kim, W. S., Wu, B. J., Suarna, C., Quinn, C. M., Rye, K. A., Stocker, R., Jessup, W. and Garner, B. (2007) Inhibition of atherosclerosis by the serine palmitoyl transferase inhibitor myriocin is associated with reduced plasma glycosphingolipid concentration. Biochem. Pharmacol. **73**, 1340–1346
21 Glaros, E. N., Kim, W. S., Quinn, C. M., Jessup, W., Rye, K. A. and Garner, B. (2008) Myriocin slows the progression of established atherosclerotic lesions in apolipoprotein E gene knockout mice. J. Lipid Res. **49**, 324–331
22 Park, T. S., Rosebury, W., Kindt, E. K., Kowala, M. C. and Panek, R. L. (2008) Serine palmitoyltransferase inhibitor myriocin induces the regression of atherosclerotic plaques in hyperlipidemic ApoE-deficient mice. Pharmacol. Res. **58**, 45–51
23 Park, T. S., Panek, R. L., Rekhter, M. D., Mueller, S. B., Rosebury, W. S., Robertson, A., Hanselman, J. C., Kindt, E., Homan, R. and Karathanasis, S. K. (2006) Modulation of lipoprotein metabolism by inhibition of sphingomyelin synthesis in ApoE knockout mice. Atherosclerosis **189**, 264–272
24 Chalfant, C. E. and Spiegel, S. (2005) Sphingosine 1-phosphate and ceramide 1-phosphate: expanding roles in cell signaling. J. Cell Sci. **118**, 4605–4612
25 Kihara, A., Mitsutake, S., Mizutani, Y. and Igarashi, Y. (2007) Metabolism and biological functions of two phosphorylated sphingolipids, sphingosine 1-phosphate and ceramide 1-phosphate. Prog. Lipid Res. **46**, 126–144

26 Hannun, Y. A. and Obeid, L. M. (2008) Principles of bioactive lipid signalling: lessons from sphingolipids. Nat. Rev. Mol. Cell Biol. **9**, 139–150
27 Pyne, S., Chapman, J., Steele, L. and Pyne, N. J. (1996) Sphingomyelin-derived lipids differentially regulate the extracellular signal-regulated kinase 2 (ERK-2) and c-Jun N-terminal kinase (JNK) signal cascades in airway smooth muscle. Eur. J. Biochem. **237**, 819–826
28 Dragusin, M., Wehner, S., Kelly, S., Wang, E., Merrill, Jr, A. H., Kalff, J. C. and van Echten-Deckert, G. (2006) Effects of sphingosine-1-phosphate and ceramide-1-phosphate on rat intestinal smooth muscle cells: implications for postoperative ileus. FASEB J. **20**, 1930–1932
29 Beers, A., Haas, M. J., Wong, N. C. and Mooradian, A. D. (2006) Inhibition of apolipoprotein AI gene expression by tumor necrosis factor α: roles for MEK/ERK and JNK signaling. Biochemistry **45**, 2408–2413
30 Rentz, S. S., Showker, J. L., Meredith, F. I. and Riley, R. T. (2005) Inhibition of sphingolipid biosynthesis decreases phosphorylated ERK2 in LLC-PK1 cells. Food Chem. Toxicol. **43**, 123–131
31 Klaunig, J. E., Goldblatt, P. J., Hinton, D. E., Lipsky, M. M., Chacko, J. and Trump, B. F. (1981) Mouse liver cell culture. I. Hepatocyte isolation. In Vitro **17**, 913–925
32 Hojjati, M. R. and Jiang, X. C. (2006) Rapid, specific, and sensitive measurements of plasma sphingomyelin and phosphatidylcholine. J. Lipid Res. **47**, 673–676
33 Garner, B. (2008) Myriocin as an atherosclerosis inhibitor. Future Lipidol. **3**, 221–224
34 Glaros, E. N., Kim, W. S., Rye, K. A., Shayman, J. A. and Garner, B. (2008) Reduction of plasma glycosphingolipid levels has no impact on atherosclerosis in apolipoprotein E-null mice. J. Lipid Res. **49**, 1677–1681
35 Bietrix, F., Lombardo, E., van Roomen, C., Ottenhoff, R., Groen, A. K. and Aerts, J. (2009) Inhibition of glycosphingolipid synthesis strongly reduces atherosclerosis development in APOE*3 Leiden mice. Atherosclerosis Suppl. **10**, e475
36 Wong, N. C. (2007) Novel therapies to increase apolipoprotein AI and HDL for the treatment of atherosclerosis. Curr. Opin. Investig. Drugs **8**, 718–728
37 Casey, D. E. (2004) Dyslipidemia and atypical antipsychotic drugs. J. Clin. Psychiatry **65**, 27–35
38 Birkenaes, A. B., Birkeland, K. I., Engh, J. A., Faerden, A., Jonsdottir, H., Ringen, P. A., Friis, S., Opjordsmoen, S. and Andreassen, O. A. (2008) Dyslipidemia independent of body mass in antipsychotic-treated patients under real-life conditions. J. Clin. Psychopharmacol. **28**, 132–137
39 La, Y. J., Wan, C. L., Zhu, H., Yang, Y. F., Chen, Y. S., Pan, Y. X., Feng, G. Y. and He, L. (2007) Decreased levels of apolipoprotein A-I in plasma of schizophrenic patients. J. Neural Transm. **114**, 657–663
40 Pereira, A., Fink, G. and Sundram, S. (2009) Clozapine-induced ERK1 and ERK2 signaling in prefrontal cortex is mediated by the EGF receptor. J. Mol. Neurosci. **39**, 185–198
41 Tedesco-Silva, H., Mourad, G., Kahan, B. D., Boira, J. G., Weimar, W., Mulgaonkar, S., Nashan, B., Madsen, S., Charpentier, B., Pellet, P. and Vanrenterghem, Y. (2004) FTY720, a novel immunomodulator: efficacy and safety results from the first phase 2A study in *de novo* renal transplantation. Transplantation **77**, 1826–1833
42 Klingenberg, R., Nofer, J. R., Rudling, M., Bea, F., Blessing, E., Preusch, M., Grone, H. J., Katus, H. A., Hansson, G. K. and Dengler, T. J. (2007) Sphingosine-1-phosphate analogue FTY720 causes lymphocyte redistribution and hypercholesterolemia in ApoE-deficient mice. Arterioscler. Thromb. Vasc. Biol. **27**, 2392–2399
43 Nofer, J. R., Bot, M., Brodde, M., Taylor, P. J., Salm, P., Brinkmann, V., van Berkel, T., Assmann, G. and Biessen, E. A. (2007) FTY720, a synthetic sphingosine 1 phosphate analogue, inhibits development of atherosclerosis in low-density lipoprotein receptor-deficient mice. Circulation **115**, 501–508

Received 3 September 2009/14 December 2009; accepted 26 January 2010
Published as Immediate Publication 26 January 2010, doi:10.1042/CS20090452